



HAL
open science

Catalyst Complexity in a Highly Active and Selective Wacker-Type Markovnikov Oxidation of Olefins with a Bioinspired Iron Complex

Jonathan Trouvé, Khalil Youssef, Sitthichok Kasemthaveechok, Rafael Gramage-Doria

► To cite this version:

Jonathan Trouvé, Khalil Youssef, Sitthichok Kasemthaveechok, Rafael Gramage-Doria. Catalyst Complexity in a Highly Active and Selective Wacker-Type Markovnikov Oxidation of Olefins with a Bioinspired Iron Complex. *ACS Catalysis*, 2023, 13, pp.4421-4432. 10.1021/acscatal.3c00593 . hal-04040460

HAL Id: hal-04040460

<https://univ-rennes.hal.science/hal-04040460>

Submitted on 22 Mar 2023

HAL is a multi-disciplinary open access archive for the deposit and dissemination of scientific research documents, whether they are published or not. The documents may come from teaching and research institutions in France or abroad, or from public or private research centers.

L'archive ouverte pluridisciplinaire **HAL**, est destinée au dépôt et à la diffusion de documents scientifiques de niveau recherche, publiés ou non, émanant des établissements d'enseignement et de recherche français ou étrangers, des laboratoires publics ou privés.

Catalyst Complexity in a Highly Active and Selective Wacker-Type Markovnikov Oxidation of Olefins with a Bio-Inspired Iron Complex

Jonathan Trouvé, Khalil Youssef, Sitthichok Kasemthaveechok, and Rafael Gramage-Doria*

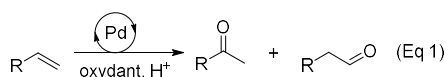
Univ Rennes, CNRS, ISCR-UMR6226, F-35000 Rennes, France

KEYWORDS ketones, olefins, iron, hydrides, Wacker

ABSTRACT: Palladium-catalyzed Wacker-type reactions occupy a central place in organic synthesis with important implications in industry. Pursuing more benign protocols by replacing palladium by first-row transition metals allowed the identification of iron as a privileged one in the last years. Although the anti-Markovnikov selectivity for iron catalysts is well developed, the Markovnikov-selective reactions still afford significant quantities of alcohol side-products and identification of reaction intermediates remains elusive so far. Herein, we present an iron catalyst that affords Markovnikov ketone products from (hetero)aromatic and aliphatic olefins in up to 99% selectivity under ambient conditions with 190,000 turnover numbers and turnover frequencies of 74 h⁻¹ at 50 °C. The catalyst design is based on the promiscuous activity encountered in the family of the cytochromes P-450 enzymes and it enables the formation of iron-hydride species under catalytically relevant reaction conditions. Substrate scope assessment and mechanistic investigations suggest that the Markovnikov-selective catalytic cycle competes with unprecedented three additional catalytic cycles (alcohol formation, hydrogenation and reductive homo-coupling) depending on the nature of the olefin and the reaction conditions.

INTRODUCTION

Since the seminal contribution by Smidt and co-workers in 1959 demonstrating the ability of palladium catalysts to oxidize olefins into carbonyl-containing products,¹ tremendous efforts have been devoted to understand, apply and improve the efficiency of this reaction.² In this respect, the development of the palladium-catalyzed production of acetaldehyde from ethylene by the Wacker company in the 1960's remains a major breakthrough in view of the industrial implementation.³ The last decades have witnessed impressive research aiming at (i) circumventing the issues associated to the harsh reaction conditions that make functional groups incompatible (searching for milder reaction conditions by avoiding chlorides, copper salts and acids)⁴ as well as (ii) disclosing palladium catalysts by ligand design to selectively control the Markovnikov or anti-Markovnikov products, that is, the ketone or the aldehyde when starting from a terminal olefin (Scheme 1).⁵



Scheme 1. General palladium-catalyzed Wacker-type oxidation of olefins.

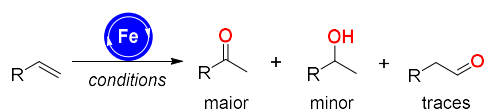
Alternatively, developing oxidation methodologies with metal catalysts derived from the first row appear promising from a sustainable point of view.⁶ Owing to the almost perfect atom-economy, Wacker-type reactions have been the subject of study for replacing the scarce palladium catalyst by more abundant and less toxic metal complexes.⁷ From

the many ones studied, iron complexes were found efficient for the anti-Markovnikov selective production of aldehydes starting from olefins as pioneered by Che using highly-sophisticated iron(III)-porphyrin catalysts.⁸ Remarkably, Arnold and co-workers engineered by directed evolution a heme-containing enzyme that affords anti-Markovnikov products under ambient pressure and thousands of turnover numbers (TONs).^{9a,b} Similar anti-Markovnikov selectivity was achieved by Lei and co-workers with water as the oxygen source by combining photocatalysis and proton-reduction catalysis.^{9c} Methodologies leading to Markovnikov ketone products have been pioneered by the groups of Han and Knölker, independently, in the presence of hydrosilanes as the hydrogen source (**Figure 1**, top).¹⁰ Notably, Knölker and co-workers demonstrated that iron(III) catalysts can operate under air at room temperature provided that dibenzoylmethanato (dbm), neocuproine or perfluorinated porphyrin ligands were employed.^{10e,f} However, variable amounts of alcohols or aldehydes are still formed depending on the nature of the starting olefin substrates and the reaction conditions (**Figure 1**, top).¹⁰

Interestingly, some contributions dealing with the use of heme-containing cytochromes P-450 for oxidation chemistry reported the trace formation of carbonyl-containing by-products besides the more common and expected hydroxylated products.¹¹ The promiscuous activity of these enzymes inspired us to study a series of iron(III)-porphyrin complexes containing peripheral carboxylic acid groups, similar to the enzymatic heme active site,¹² as prospective catalysts for Wacker-type reactions (**Figure 1**, bottom). Whereas the remote carboxylic acid groups belonging to

heme-containing porphyrins are relevant for several biological purposes,³ we anticipated that they could be taken as a benefit for increasing the electronegativity character of the catalytically active iron center,¹⁴ and thus stabilize otherwise inaccessible reaction intermediates in Wacker-type iron-catalyzed oxidations. Herein, we demonstrate that the iron(III) complex **Fe-1** containing the carboxylic acid functionalities located in *para* position of the *meso* phenyl groups¹⁵ behaved as a highly active catalyst for the Markovnikov-selective production of ketones from olefins in the presence of hydrosilanes as reagents and an oxygen source (air or dioxygen) with up to unprecedented 190,000 TONs and 74 h⁻¹ of TOF (**Figure 1**, bottom). Moreover, kinetic studies and unexpected identification of by-products for some types of unbiased olefins revealed the complexity of the catalysis with multiple catalytic cycles being operative to some extent. Such fundamental mechanistic understanding allowed the careful selection of reaction conditions that suppressed the undesired side reactions. In addition, we provide for the first time spectroscopic evidences for the formation of the so far elusive iron-hydride species, which has been postulated as key intermediate previously.¹⁰

Markovnikov-selective Iron-catalyzed Wacker-type oxidation of olefins:



Han (2017): FeCl ₂ (10 mol%) PMHS (3 equiv) EtOH, 80 °C, air	Knölker (2018): FePcF ₁₆ (5 mol%) Et ₃ SiH (2 equiv) EtOH, r.t., O ₂	Knölker (2021): Fe(dbm) ₃ (3 mol%) or FeCl ₂ + neocuproine (3 mol%) or (FeTPPF ₂₈) ₂ O (2.5 mol%) PhSiH ₃ , EtOH, r.t., air
--	--	---

This work:

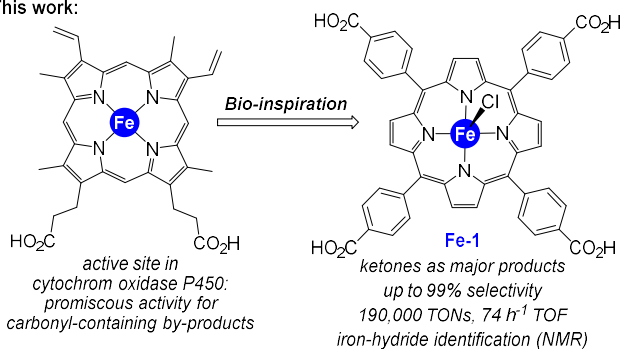


Figure 1. State-of-the-art for the Markovnikov-selective iron-catalyzed Wacker-type oxidation of olefins (top) and current bio-inspired approach (bottom). PMHS = polymethylhydrosiloxane, FePcF₁₆ = hexadecafluorinated iron-phthalocyanine, dbm = dibenzoylmethanato, FeTPPF₂₈ = octacosafuoro-tetraphenyl-iron-porphyrine.

RESULTS AND DISCUSSION

Initial catalytic assessment

Firstly, the oxidation of 4-*tert*-butylstyrene (**1a**) was evaluated as a model reaction under a set of reaction conditions similar to those reported by Han and Knölker,¹⁰ that is, in the presence of Et₃SiH and O₂ atmosphere in ethanol solvent (**Table 1**).¹⁶ By using the iron(III)-porphyrin complex **Fe-1** in 7.5 mol% catalyst loading under O₂ atmosphere, full conversion of starting material was reached after 18 hours with 98% selectivity towards the formation of the ketone product **2a** resulting from Markovnikov selectivity (**Table 1**, entry 1). The remaining 2% corresponded to the alcohol by-product **3a** and no aldehyde was detected. The influence of the ligand is remarkable for this type of reaction since bearing the carboxylic acid units in *meta* or *ortho* position of the *meso*-substituted phenyl groups decreased the conversion to 90% and 29%, respectively, while keeping similar levels of alcohol by-products.¹⁶ When using the carboxylic ester version of **Fe-1**, that is replacing all four CO₂H groups by CO₂Me groups, no activity was encountered (**Table S1** in the Supporting Information).¹⁶ This observation indicates that (i) the degree of solubility of the iron catalyst in the media has little impact in this catalysis because the acid-containing iron porphyrin is less soluble than the ester counterpart, and (ii) the iron active species is likely stabilized by electronwithdrawing groups such as CO₂H. These observations are complementary to Knölker's systems, in which the reactivity of the iron complex is correlated to their solubility, being necessary to use perfluorinated ligands.^{10c-f}

Importantly, we noted that the water content in the ethanol solvent has a major impact on the outcome of the catalysis (**Table S2** in the Supporting Information).¹⁶ In the range from 0 to 10% volume content, we identified 4% as the suitable amount of water, which corresponds to the commercially supplied ethanol. Higher content of water increased the amount of alcohol by-product (**Table 1**, entry 2-3), whereas lower amounts affected the overall conversion (**Table 1**, entries 4-5). Other solvents were not compatible (**Table S3** in the Supporting Information).¹⁶ Consequently, the influence of water has a clear effect on the formation of alcohol by-product. Interestingly, it was possible to reduce the loading of both the iron catalyst to 2.5 mol% and the hydrosilane reagent to 2 equivalents while keeping an excellent reactivity and selectivity (**Table 1**, entry 6). Decreasing the catalyst loading to 1.5 mol% led to a modest 73% conversion (**Table 1**, entry 7). The catalysis was similarly efficient when switching O₂ by air (**Table 1**, entries 8-9) and a kinetic experiment revealed a direct correlation between product formed and substrate consumed (Figures S1-S2 in the Supporting Information).¹⁶ For comparison purposes, a reaction was carried out replacing **Fe-1** by FeCITPP (TPP = tetraphenylporphyrin) (**Table 1**, entry 10) and by a combination of FeCITPP and benzoic acid (**Table 1**, entry 11). In both cases, a very poor reactivity was encountered and the starting material **1a** was almost unconsumed, thus highlighting the relevance of covalently-linking the carboxylic acid groups to the iron-porphyrin backbone in

Fe-1. To verify whether the reaction involved formation of transient radical species as known for similar iron catalysts,¹⁰ we performed a catalytic reaction in the presence of TEMPO [TEMPO = (2,2,6,6-tetramethylpiperidin-1-yl)oxyl] as a radical trapping agent (Table 1, entry 12). In this case, the reactivity was fully suppressed, thereby supporting the formation of radicals in the catalytic cycle.

Table 1. Evaluation of the reaction conditions for the Fe-1-catalyzed oxidation of 4-*tert*-butylstyrene.^[a]

Entry	Deviation from above reaction conditions	Conv. (%) ^[b]	Yield 2a (%) ^[b]	Yield 3a (%) ^[b]
1 ^[c]	none	>99	98	2
2	10% water content	>99	92	8
3	6% water content	>99	91	9
4	2% water content	86	82	4
5	0.2% water content	60	57	3
6 ^[d]	Fe-1 (2.5 mol%), Et ₃ SiH (2 equiv)	>99	98	2
7 ^[d]	Fe-1 (1.5 mol%), Et ₃ SiH (2 equiv)	73	64	9
8 ^[d]	as entry 6 and air instead of O ₂	95	90	5
9	as entry 8 and 48 hours	>99	93	7
10 ^[e]	FeCITPP instead of Fe-1	<5	<5	n.d.
11	as entry 10 with PhCO ₂ H (20 mol%)	<10	<10	n.d.
12	with TEMPO (1 equiv)	0	0	0
13	with K ₂ CO ₃ or NEt ₃ (30 mol%)	0	0	0

[a] Reaction conditions: **1a** (0.325 mmol), Et₃SiH (0.975 mmol), Fe-1 (7.5 mol%), undistilled EtOH (3 mL), O₂ (1 bar, balloon), r.t., 18 hours. [b] Conversion and yields determined by GC and GC-MS using dodecane as internal standard. [c] Water content in commercial EtOH is 4% in volume. [d] 24 hours instead of 18 hours. [e] Reaction conditions: **1a** (0.325 mmol), Et₃SiH (0.975 mmol), FeTPP (5 mol%), EtOH (3 mL), air, r.t., 24 hours. TPP = tetraphenylporphyrin. n.d. = not determined.

Furthermore, the reaction did not proceed in the presence of inorganic or organic bases such as potassium carbonate (K₂CO₃) or triethylamine (NEt₃) that can deprotonate the carboxylic acid groups from the iron catalyst (Table 1, entry 13). In these basic conditions, a biphasic system is present with the concentrated aqueous layer containing the dark violet iron catalyst and the ethanolic layer slightly yellowish without the iron catalyst. This observation was taken as an advantage to explore a proof-of-concept temporal control of reactivity by sequential addition of base and acid (Figure 2). The catalysis was executed under standard conditions and after one hour, NEt₃ was added to shut down the activity because the iron complex appears as insoluble tetracarboxylate species (note: adding K₂CO₃

or NEt₃ results in an exothermic reaction). Addition of trifluoroacetic acid (TFA) after two hours solubilized again the iron catalyst, thereby restoring the activity of the catalyst with the same levels of ketone selectivity. The careful and precise addition of both organic base (30 mol%) and organic acid (50 mol%), respectively, is critical for the observed temporal control of reactivity.¹⁶

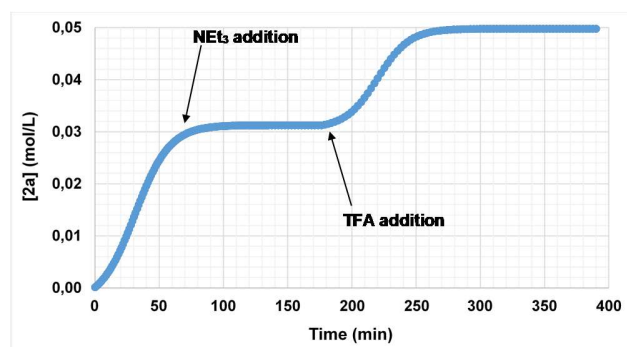
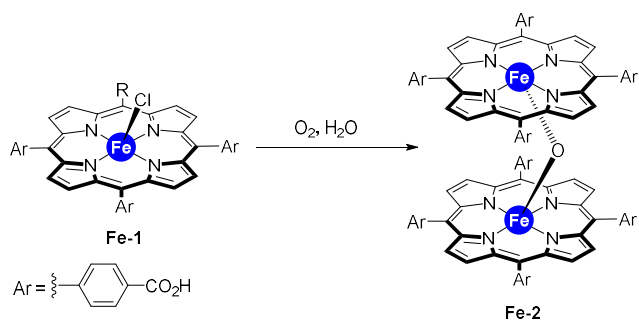


Figure 2. Temporal control of the reactivity in the iron-catalyzed Wacker-type oxidation of olefin **1a** by in situ addition of NEt₃ base and TFA acid. Reaction conditions derived from Table 3, entry 1 (*vide infra*).

From catalyst deactivation to catalyst outperformance

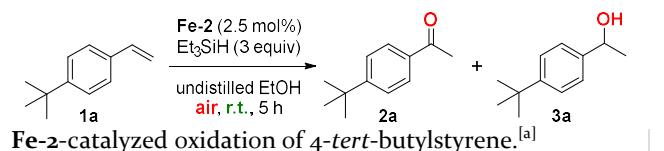
Unexpectedly, we realized that samples of Fe-1 that were stored under air atmosphere were inactive in catalysis when applying the optimal reaction conditions (Table 1, entries 1, 6, 8 and 9) after some time. Indeed, HRMS (MALDI) studies unambiguously revealed the presence of a μ -oxo-bridged diiron species Fe-2 (m/z for C₉₆H₅₆N₈O₁₇⁵⁶Fe₂ 1704.263 ± 12 ppm) derived from Fe-1 that was formed upon prolonged standing under ambient air (Scheme 2 and Figure S3 in the Supporting Information).¹⁶ The formation of similar dimeric species from H₂O and/or O₂ with iron-porphyrins is well-known.^{17,18} It is worthy to note at this stage, that Knölker and co-workers did identify μ -oxo-bridged diiron species with perfluorinated phthalocyanine and perfluorinated porphyrine ligand, respectively, as selective catalysts for Markovnikov-selective oxidation of olefins in the presence of hydrosilanes (i.e. Et₃SiH, Ph₃SiH, PhSiH₃, etc.) as hydrogen source.^{10c,d,f} In stark contrast, Fe-1 does form thermodynamically stable dimeric species that cannot be cleaved by Et₃SiH, strongly suggesting that dimers are not involved in the catalytic cycle for the oxidation of olefins into ketones using the bio-inspired Fe-1 catalyst. In fact, the formation of dimeric species might be considered as an off cycle intermediate for the current case of study.



Scheme 2. Formation of μ -oxo-bridged diiron species **Fe-2** from **Fe-1** upon prolonged standing under ambient conditions.

In order to avoid undesired catalyst inhibition pathways *via* formation of μ -oxo-bridged dimeric species, we evaluated the influence of the nature of the hydrosilane reagent in the catalytic outcome when using **Fe-2** as a precatalyst under air atmosphere (**Table 2**). As stated above, the oxidation reaction using Et_3SiH with the dimer **Fe-2** led to negligible conversion of substrate **1a** and formation of traces of ketone **2a** (**Table 2**, entry 1). Similar poor results were obtained by employing Ph_3SiH and PMHS (**Table 2**, entries 2-3). However, the reactivity and selectivity was fully recovered when using Ph_2SiH_2 or PhSiH_3 as reagents, respectively (**Table 2**, entries 4-5). Remarkably, the reactions were shortened to 5 hours whereas alcohols by-products raised to 8-9%, values that outperform state-of-the-art systems.¹⁰ In order to better understand this unexpected catalyst deactivation *via* dimer formation, we studied the feasibility of *in situ* catalyst activation starting from **Fe-2** as the catalyst in the presence of unreactive Et_3SiH (**Table 2**, entry 1) provided that catalytic quantities of PhSiH_3 are present to cleave the dimer (**Table 2**, entry 6-7). In fact, under unreactive conditions, the addition of 10 mol% of PhSiH_3 led to 43% conversion of olefin **1a** into ketone **2a** in a selective manner (**Table 2**, entry 6). As expected, raising the PhSiH_3 loading to 20 mol% in the presence of 2 equivalents of Et_3SiH afforded the ketone product in 98% yield (**Table 2**, entry 7), thereby demonstrating that the catalysis at play with Et_3SiH does not involve formation of dimeric iron species. Other additives were evaluated in order to cleave the dimeric iron structure **Fe-2** into the catalytically active monomeric **Fe-1**. For instance, HCl as additive proved successful for this purpose although leading to a modest yield of *ca.* 50% of ketone **2a** (**Table 2**, entries 8-9). These findings indicate that fine-tuning reaction conditions may lead to the formation of the active **Fe-1** species with a rather cheap and affordable Brønsted acid in catalytic amounts.

Table 2. Optimization of the reaction conditions for the



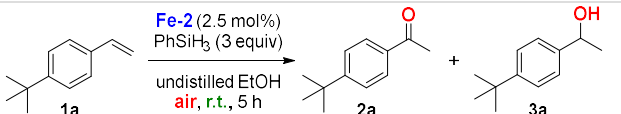
Entry	Deviation from above reaction conditions	Conv. (%) ^[b]	Yield 2a (%) ^[b]	Yield 3a (%) ^[b]
1 ^[c]	none	<5	<5	n.d.
2	with Ph_3SiH instead of Et_3SiH	<5	<5	n.d.
3	with PMHS instead of Et_3SiH	<5	<5	n.d.
4	with Ph_2SiH_2 instead of Et_3SiH	>99	91	9
5	with PhSiH_3 instead of Et_3SiH	>99	92	8
6	with PhSiH_3 (10 mol%)	43	43	n.d.
7	with PhSiH_3 (20 mol%)	>99	98	2
8	with HCl (10 mol%)	60	48	12
9	with HCl (20 mol%)	62	49	13

[a] Reaction conditions: **1a** (0.325 mmol), Et_3SiH (0.975 mmol), **Fe-2** (2.5 mol%), EtOH (3 mL), air, r.t., 5 hours. [b] Conversion and yields determined by GC and GC-MS using dodecane as internal standard. [c] Water content in commercial EtOH is 4% in volume. n.d. = not determined.

Having established the unique activation mode of the iron pre-catalyst **Fe-2** in the presence of PhSiH_3 as the reductant (**Table 2**, entry 5 and 7), we further studied the potential of the present catalyst regarding catalyst stability, reactivity, selectivity and recyclability. In fact, by reducing the catalyst loading to 1.25 mol%, still full conversion of **1a** and 92% yield of ketone **2a** was obtained (**Table 3**, entries 1-2). However, decreasing the number of equivalents of PhSiH_3 by half led to 10% remaining of starting material while keeping an excellent Markovnikov selectivity (**Table 3**, entry 3). As it was observed for the pre-catalyst **Fe-1** (**Table 1**, entries 1-5), the amount of water also influenced the catalytic outcome observed when employing the pre-catalyst **Fe-2**. For instance, by reducing the water content in the media from 4% to 0.2% in volume, the conversion of **1a** and yield of ketone **2a** dropped by half after 12 hours (**Table 3**, entry 4). Consequently, water plays a critical role for determining the Markovnikov-selective oxidation process regardless of the choice of silane reagent, thereby indicating a possible role in the catalytic cycle, but not as hydrogen source since no deuterium was incorporated in the ketone product when employing deuterated solvents ($\text{EtOH}/\text{D}_2\text{O}$ and $\text{MeOD}/\text{D}_2\text{O}$). Additional kinetic experi-

ments revealed that the substrate (**1a**) consumption is directly related to the formation of the Markovnikov ketone product **2a** at different catalyst concentrations (see Figures S4-S8 in the Supporting Information).¹⁶ The pseudo-first order in catalyst strongly supports formation of monomeric species throughout the whole catalytic cycle. As observed by Knölker for other iron-catalyzed Wacker-type oxidation of olefins,^{10c-10f} alcohol **3a** is not here an intermediate because using **3a** as the substrate led to no ketone formation with full recovery of the starting material (Table 3, entry 5). The temperature range was assessed and the reaction was operative even at challenging 0 °C with 40% yield of ketone **2a** after 5 hours (Table 3, entry 6). To the best of our knowledge, this is the first example in which a transition metal catalyzed Wacker-type oxidation of olefins is reported to work at such low temperature. The catalysis performed at 50 °C was less efficient with 70% yield of **2a** (Table 3, entry 7) although more than a six-fold rate acceleration was reached when compared to the reaction at 0 °C (see Figure S18 and Table S9 in the Supporting Information).^{16,19} Kinetic studies following on time both substrate and silane consumption as well as ketone formation established that the reaction at 50 °C reached a plateau at one hour with complete silane consumption (see Figures S11-S13 in the Supporting Information).¹⁶ This unexpected silane degradation was catalyzed by the iron catalyst since no silane consumption was observed in the absence of **Fe-2** or **Fe-1** under catalytically relevant conditions.¹⁶ Interestingly, we disclosed an intriguing dilution effect since the catalysis was faster (3 hours) when performed in a two times more diluted media (Table 3, entry 8). Under this reaction condition, decreasing the catalyst loading to 1.25 mol% did not influence the selectivity although the reaction required 8 hours for completion (Table 3, entry 9). Additional control experimentation highlighted the need of all reagents for the success of the transformation (Table 3, entries 10-11) and that the O₂ from air is the oxidant for this transformation (Table 3, entry 12).

Table 3. Evaluation of the reaction conditions for the **Fe-2**-catalyzed oxidation of *tert*-butylstyrene in the presence of PhSiH₃.^[a]



Entry	Deviation from above reaction conditions	Conv. (%) ^[b]	Yield 2a (%) ^[b]	Yield 3a (%) ^[b]
1 ^[c]	none	<99	92	8
2 ^[d]	with Fe-2 (1.25 mol%)	<99	92	8
3 ^[e]	as entry 2, with PhSiH ₃ (1.5 equiv)	90	85	5
4 ^[e]	with dry EtOH (0.2% water content)	51	47	4
5	3a as substrate instead of 1a	0	0	0
6	0 °C instead of r.t.	40	40	n.d.
7	50 °C instead of r.t.	75	70	5
8	with undistilled EtOH (6 mL), 3 h	<99	92	8
9 ^[d]	as entry 8 with Fe-2 (1.25 mol%)	<99	92	8
10	absence of PhSiH ₃	0	0	0
11	absence of Fe-2	0	0	0
12	Argon instead of air	0	0	0

[a] Reaction conditions: **1a** (0.325 mmol), Et₃SiH (0.975 mmol), **Fe-2** (2.5 mol%), EtOH (3 mL), air, r.t., 5 hours. [b] Conversion and yields determined by GC and GC-MS using dodecane as internal standard. [c] Water content in commercial EtOH is 4% in volume. [d] 8 hours of reaction time. [e] 12 hours of reaction time. n.d. = not determined.

Moreover, the **Fe-2** pre-catalyst is a platform compatible to study temporal control of catalysis by *in situ* switching the atmosphere of the reaction as a chemical stimuli (Figure 3). In addition, the robustness of such catalysis was exemplified by using as low as 1 ppm catalyst loading of **Fe-2** (Scheme 3). At room temperature and after 48 hours, a TON value of 32,500 was reached (TOF = 26 h⁻¹) and it increased to 190,000 (TOF = 74 h⁻¹) when the reaction was carried out at 50 °C. Such values of TON and TOF are the largest so far reported for iron-catalyzed Wacker-type oxidation of olefins into ketones. Interestingly, when using 1 ppm of iron catalyst at 50 °C, we noted that the silane reagent did not decompose even after reaching the highest TON value. This contrasts when using higher catalyst loadings in which the silane readily decomposes into siloxanes at the end of the reaction.

Because of the presence of carboxylic acid groups present in the iron catalyst, we tested, as a proof of concept, the possibility to recover the iron catalyst by trival acid/base treatment and precipitation (see Table S13 in the Supporting Information).¹⁶ Indeed, it was possible to perform up to 2 runs with the recycled iron catalyst while keeping similar levels of reactivity (full conversion of olefin **1a** in less than 5 hours) and selectivity (>92% yield of ketone **2a**).¹⁶

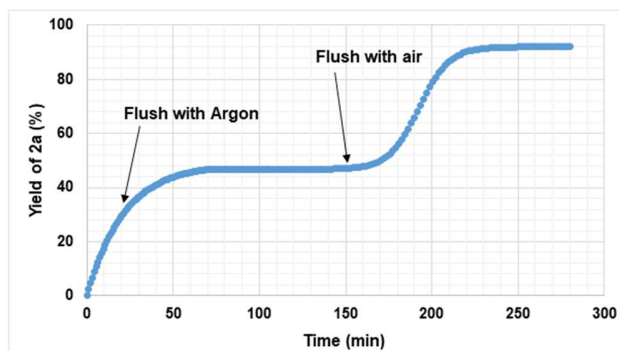
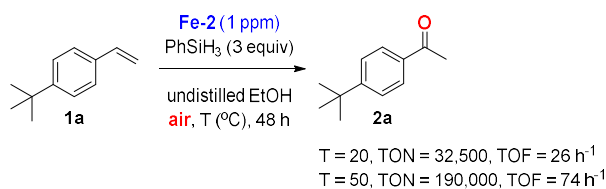


Figure 3. Temporal control of the reactivity in the iron-catalyzed Wacker-type oxidation of olefin **1a** by switching the atmosphere from air to argon under two cycles. Reaction conditions derived from **Table 3**, entry 1.

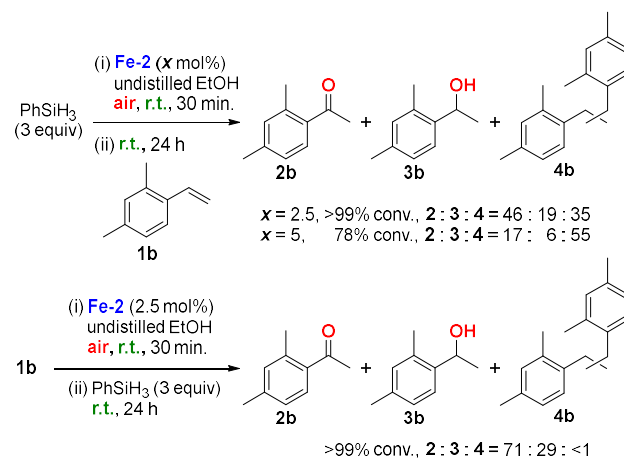


Scheme 3. Search for the highest TON and TOF in the iron-catalyzed Wacker-type oxidation of 4-*tert*-butylstyrene.

Circumventing unexpected side-reactions and substrate scope evaluation

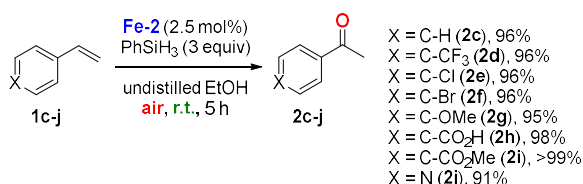
The formation of alcohol side-product **3a** for the oxidation of 4-*tert*-butylstyrene (**1a**) was reduced to a residual 2% (**Table 1**, entry 1 and 6; and **Table 2**, entry 7), which is remarkable as regards of literature precedents.¹⁰ Intriguingly, we noted that the order of addition of reagents plays a key role in the product selectivity as illustrated for the case of the olefin **1b** (**Scheme 4**). Besides the formation of the desired ketone (**2b**) and alcohol (**3b**) side-product, compounds such as **4b** resulting from a reductive homocoupling were formed in significant quantities (up to 55%) when the olefin substrate was introduced as the last component to the reaction mixture (**Scheme 4**, top). In this case, the formation of **4b** may follow a mechanism involving radical hydrogen atom transfer²⁰ as discussed by the breakthrough contributions by Baran on iron-catalyzed olefin functionalization,^{21a-d} and by others later.^{21e-k} Alternatively, by adding the silane PhSiH₃ reagent as the very last component to the reaction mixture, the side-product **4b** was reduced to trace amounts (<1%) with the targeted ketone formed in 71% yield (**Scheme 4**, bottom), which is notable considering the steric and electronics effects that make substrate **1b** prone to stabilize different benzylic radical intermediates (*vide infra*).^{10,21} The variation of the chemo-selectivity of the iron-catalyzed reaction depending

on the order of addition of reagents was a general trend for most of the aryl olefins tested (see Figure S19 in the Supporting Information).¹⁶



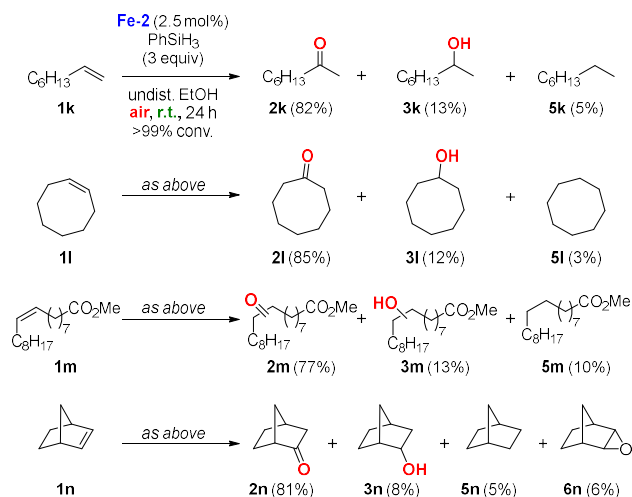
Scheme 4. Experimentation highlighting the impact of the order of addition of the reagents in the product selectivity of the Fe-2-catalyzed Wacker-type oxidation of 2,4-dimethylstyrene (product **4b** exists as a mixture of branched isomers). Reaction conditions: (i) **1** (0.325 mmol), Fe-2 (2.5 mol%), EtOH (3 mL), air, r.t., 30 min (ii) PhSiH₃ (0.975 mmol), air, r.t. 4.5 hours. GC yields reported after performing at least 3 experiments.²²

After a careful search of the optimal reaction conditions, we evaluated the olefin scope of the Fe-2-catalyzed Wacker-type oxidation. In the case of aryl olefins as the substrates, the reactions were completed in less than five hours under ambient conditions of pressure and air (**Scheme 5**). The tolerance of the catalytic system made possible the use of different functional groups including aryl, alkyl, halides (fluoride, chloride and bromide), ethers, and carboxylic acids (**2c-h**). In all cases, the alcohol side-products did not reach more than 5%, which outperforms previous reports.¹⁰ Importantly, the reaction was compatible with ester groups affording exclusively the ketone product **2i** (99% selectivity) with no detectable formation of alcohol side-product. The catalysis was also compatible with pyridine heterocycles affording the corresponding ketone product **2j** in 91% yield at room temperature in 5 hours with no formation of *N*-oxide species, which strikingly contrasts with the previously reported conditions (85% at 80 °C in 12 hours).^{10a} This iron-catalyzed protocol outperforms current state-of-the-art iron catalysts in terms of activity and selectivity.



Scheme 5. Evaluation of (hetero)aryl olefins in the **Fe-2**-catalyzed Wacker-type oxidation. Reaction conditions: (i) **1** (0.325 mmol), **Fe-2** (2.5 mol%), EtOH (3 mL), air, r.t., 30 min (ii) PhSiH₃ (0.975 mmol), air, r.t. 4.5 hours. GC yields reported after performing at least 3 experiments for each substrate.²²

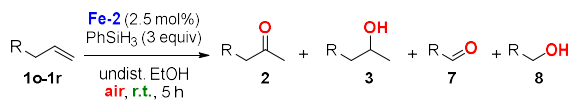
Next, we enlarged the substrate scope to purely aliphatic olefins, which are much less reactive than the aryl ones (**Scheme 6**). Indeed, precedents in the literature indicate that terminal as well as internal olefins are typically reactive using a high iron catalyst loading (20 mol%),^{10a} if not, the yields did not exceed 60%.^{10e} In the present case, using **Fe-2** at 2.5 mol% catalyst loading during 24 hours under ambient conditions of pressure and temperature, 1-octene (**1k**) and *cis*-cyclooctene (**1l**) substrates did afford the ketone products **2k** and **2l** resulting from Markovnikov selectivity in a remarkable 82% and 85% yield, respectively, whereas the alcohol side-products **3k** and **3l** formed in a range of 12–13%. Unexpectedly, side-products **5k** and **5l** resulting from hydrogenation of the starting material formed in trace amounts (3–5%). Such findings were also observed when using bio-sourced methyl oleate (**1m**) as the substrates, respectively, in which, besides the major formation of ketone product **2m** (77%), the hydrogenated side-product **5m** raised to 10%. In the case of the highly sterically congested norbornene (**1n**), the ketone product **2n** formed in an exceptional 81% yield and only 8% of alcohol **3n** and 6% of epoxyde **6n** side-products;²³ the hydrogenated side-product **5n** was only detected as traces. As such, careful analysis of the reaction mixtures revealed that, for the case of aliphatic olefins, iron-catalyzed hydrogenation pathways compete with alcohol formation as the side-products.

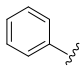
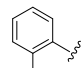
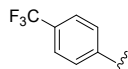
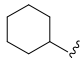


Scheme 6. Evaluation of aliphatic olefins in the **Fe-2**-catalyzed Wacker-type oxidation. Reaction conditions: (i) **1** (0.325 mmol), **Fe-2** (2.5 mol%), EtOH (3 mL), air, r.t., 30 min (ii) PhSiH₃ (0.975 mmol), air, r.t. 24 hours. GC yields reported after performing at least 3 experiments for each substrate.²²

As a follow-up series of substrates, we evaluated the reaction outcome for allyl-containing derivatives (**10–1r**, **Table 4**), which are known to undergo predominantly oxidative C=C bond cleavage to aldehydes (**7**) under iron catalysis,^{10a,24} or isomerization/oxidation tandem sequence under nickel catalysis.²⁵ For allyl-benzene derivatives **10** and **1p**, the current **Fe-2**-catalyzed methodology provides the major ketone products **20–2p** resulting from a formal Markovnikov selectivity in a promising 44–52% yields (**Table 4**, entries 1–2). Besides the expected formation of alcohol side-products (**30–3p**), the benzylic alcohols **80–8p** resulting from the hydrogenation of aldehydes (**70–7p**) were also detected (**Table 4**, entries 1–2), emphasizing the relevance of hydrogenation side-reactions for this particular type of substrates under iron catalysis. In the case of the trifluoromethoxy-substituted derivative (**1q**), the catalysis was less selective with the ketone **2q** formed in 38% yield (**Table 4**, entry 3). For this substrate, hydrogenation of the olefin double bond was observed in a non-negligible 14% yield. On the other hand, a more chemically-robust allylcyclohexane (**1r**) did not undergo any C=C bond cleavage and the ketone product **2r** was obtained in a useful 70% yield with 29% of alcohol **3r** (**Table 4**, entry 4), thereby demonstrating the importance of the aromatic fragment within **10–1q** to explain the side-products **7** and **8** resulting from benzylic fragmentation.

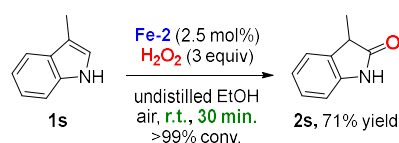
Table 4. Evaluation of allyl-containing derivatives in the Fe-2-catalyzed Wacker-type oxidation.^[a,b]



1	R	Conv. (%) ^[c]	Yield 2 (%) ^[c]	Yield 3 (%) ^[c]	Yield 7 (%) ^[c]	Yield 8 (%) ^[c]
1o		>99	52	2	11	25
1p		>99	44	10	12	27
1q		>99 ^[d]	38	18	0	28
1r		>99 ^[e]	70	29	0	0

[a] Reaction conditions: (i) **1** (0.325 mmol), Fe-2 (2.5 mol%), EtOH (3 mL), air, r.t., 30 min (ii) PhSiH₃ (0.975 mmol), air, r.t. 4.5 hours. [b] Water content in commercial EtOH is 4% in volume. [c] Conversion and yields determined by GC and GC-MS using dodecane as internal standard after performing at least 3 experiments for each substrate. [d] 14% of product resulting from olefin hydrogenation of **1q** was detected. [e] 1% of product resulting from olefin hydrogenation of **1r** was detected.

Finally, inspired by recent discoveries regarding the oxidation chemistry of indole heterocycles by heme-enzymes²⁶ and in view to replace the highly acidic and oxidizing reagents (HCl, hypervalent halides, peroxy acids, ox-one) typically employed with state-of-the-art methodologies²⁷ by more sustainable and benign protocols, we applied our iron-catalyzed methodology to indole **1s** (**Scheme 7**). Under the developed reaction conditions, full conversion was observed in only 30 minutes and the 2-ox-indole product **2s** was isolated in a non-optimized 71% yield. The reaction required H₂O₂ as the oxidant and the absence of silane, thereby suggesting that the reaction mechanism taking place here, which is beyond the scope of the current contribution, is different than that operating for aromatic and aliphatic olefins. To the best of our knowledge, this is the first use of an abiological catalyst enabling formation of 2-oxindole from indole. This type of heterocycles are privileged motifs in chemicals that display important pharmacological properties.²⁸ Note that the reaction conditions reported in **Scheme 7** failed to provide ketone **2a** starting from the aromatic olefin **1a**.

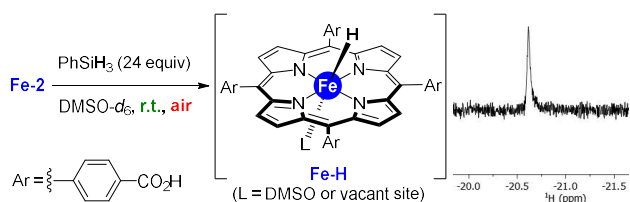


Scheme 7. Fe-2-catalyzed Wacker-type oxidation of an indole derivative. Reaction conditions: (i) **1s** (0.325 mmol), Fe-2 (2.5 mol%), H₂O₂ (0.975 mmol), EtOH (3 mL), air, r.t., 30 min.

Mechanistic insights

To the best of our knowledge, no iron-hydride species have been spectroscopically characterized in the context of Wacker-type oxidation of olefins nor iron-catalyzed reductive olefin functionalization.^{10,21} On the other hand, iron-porphyrin hydride complexes are known to form under electrocatalytic conditions in the context of the proton-to-H₂ reduction processes.²⁹ As such, we pursued the synthesis of such elusive iron-hydride Fe-H species by mixing Fe-2 with excess of PhSiH₃ in DMSO-*d*₆ (DMSO = dimethylsulfoxide) under air atmosphere and we monitored the transformation by ¹H NMR spectroscopy (**Scheme 8** and Figures S21-S27 in the Supporting Information).¹⁶ After a couple of minutes, a well-defined singlet was observed at $\delta = -20.6$ ppm (**Scheme 8**), which was assigned to a hydride signal considering previous pentacoordinated iron-hydride complexes³⁰ as well as precedent hydride complexes derived from rhodium-porphyrins that have been spectroscopically characterized.³¹ Additionally, the integrity of the porphyrin core remained intact according to the presence of NMR signals belonging to the aromatic (two doublets at $\delta = 8.39$ ppm and 8.28 ppm with ³J_{AB} = 8 Hz) as well as the pyrrolic protons (broad singlet at δ ca. 11 ppm) and the carboxylic acid protons (broad singlet at δ ca. 13 ppm). It is relevant to highlight that the pyrrolic protons undergo a massive up field shift from >70 ppm to ca. 11 ppm, thereby indicating that the addition of PhSiH₃ significantly alters the chemical environment around the iron center. We also observed formation of H₂ ($\delta = 4.6$ ppm – bubbling was observed at naked eye as well)³² and side-products resulting from PhSiH₃ degradation such as (PhSiH₂)₂O and (PhSiH-O)_n at $\delta =$ ca. 5 ppm,³³ that increase their concentration upon time. Note that in the absence of iron species, the hydride signal was not observed, appearing the chemical shift of the non-aromatic hydrogen atoms from PhSiH₃ at ca. $\delta = 4.2$ ppm values.³⁴ The formation of iron-hydride species with this bio-inspired ligand does not require the presence of EtOH as it was postulated for other iron-catalyzed Wacker-type oxidations.¹⁰ Unfortunately, because of the high sensitivity and very short lifetime of this species, it was not possible to perform additional characterization studies to quantify its formation.³⁵ Throughout the *in situ* ¹H NMR analysis, PhSiH₃ decomposed into an oligomeric/polymeric material whereas the integrity of the proton signals of the iron-porphyrin remained unaltered. However, at this stage, it is not possible to determine

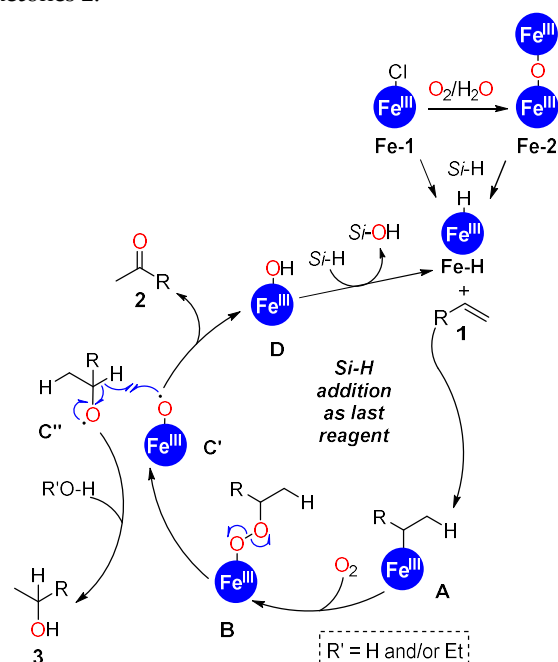
which ligands are axially coordinating to the iron center. It is relevant to note that the iron-catalyzed Wacker-type oxidation of olefin **1a** following the optimal reaction conditions reported in **Scheme 5** but in DMSO (containing H₂O 4% volume) as the solvent still afforded the corresponding ketone product **2a** in 50% yield with 60% conversion of **1a** (<5% of alcohol side-product **3a** was identified) after 24 hours at room temperature. Attempts to identify iron-hydride species with a carboxylic acid-free FeCl-tetra-phenylporphyrin with a very broad signal appeared again at δ ca. -20 ppm (Figures S28-S32 in the Supporting Information).¹⁶



Scheme 8. Transient formation of Fe-H species starting from Fe-2 in the presence of PhSiH₃ as hydride source together with the characteristic hydride signal identified by ¹H NMR spectroscopy (right).

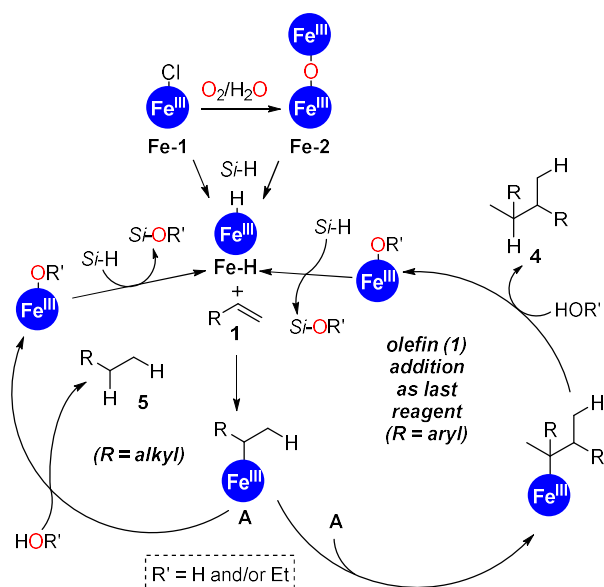
Considering the formation of iron-hydride species with our bio-inspired ligand as well as previous observations discussed in detail above and precedents in the literature,¹⁰ we propose a plausible mechanistic overview for this Wacker-type transformation in which monomeric iron species are present throughout the whole catalytic cycle with dimeric iron formation as an off cycle pathway (**Scheme 9**). The main catalytic cycle that operates when adding the silane as the last reagent is the one responsible for forming the ketone product **2** starting from the olefin starting material **1** (**Scheme 9**). Initially, iron-hydride species Fe-H form that react in a Markovnikov-selective manner with the olefin leading to Fe-alkyl intermediate **A** with addition of the hydride in the terminal carbon site. We assume the hydride to alkyl transformation occurs by an H⁺ addition. Note that the role of silane as hydride source has been elegantly demonstrated by Knölker in thorough mechanistic studies of iron-catalyzed Wacker-type oxidation of olefins.^{10c-e} Next, after oxygen reaction the iron-peroxo species **B** forms which further undergoes a radical rearrangement (species **C'** and **C''**) leading to the final ketone product **2**. The final iron-hydroxy species **D** is regenerated into the active Fe-H after reaction with a hydrosilane leading to silanols that can readily be decomposed into siloxanes,³³ as experimentally observed (*vide supra*). However, it cannot be ruled out an eventual heterolytic O-O cleavage at species **B** leading to the ketone **2** and iron-hydroxy species **D**. On the other hand, the intermediate species **C''** may undergo protonation with ethanol and/or water leading to the alcohol side-product **3**. In par-

allel, the alcohol side-product **3** can be formed from intermediate **B** via a Mukayama-type hydration mechanism.³⁶ As an additional control experiment, the pure ketone product **2a** was submitted to the optimal Wacker-type reaction conditions (see **Scheme 5**) leading to no formation of alcohol side-product **3a**, thereby establishing that the alcohols **3** are not formed via iron-catalyzed hydrogenation of ketones **2**.



Scheme 9. Postulated, simplified reaction mechanism for the iron-catalyzed Wacker-type oxidation of olefins **1** into **2** and mechanistic proposal for the formation of alcohol side-products **3**. The blue half-arrows (one-electron move) apply only to the iron-catalyzed Wacker-type oxidation of olefins **1** into **2**. The heme-like porphyrin ligand around the iron center is not depicted for the sake of clarity. Si-H stands for any silane.

For explaining the formation of side-products **4** (**Scheme 4**) resulting from reductive olefin homo-coupling and hydrogenated ones such as **5** for the challenging olefins evaluated in **Scheme 6**, a plausible mechanism is proposed in **Scheme 10**. A common intermediate iron-alkyl species **A** may form in both catalytic cycles (**Scheme 10**). Then, in the case of olefin addition as the last reagent (see discussion above), the reductive homo-coupling pathway dominates towards formation of product **4** in which both silane and ethanol are source of hydrogen atoms (**Scheme 10**, right), which is analogous to the iron-catalyzed reductive olefin functionalization chemistry.²¹ We hypothesize that an intermolecular reaction between two species such as **A** in order to explain the branched selectivity observed in **4** as well as the fact that increasing the iron catalyst loading increases the amount of side-product **4** obtained. On the other hand, species **A** may undergo protonation from the alcohol solvent leading to an iron-alkoxyde species and affording alkane side-product for the case of aliphatic olefin substrates (**Scheme 10**, left). The iron-alkoxyde species can react with a hydrosilane forming back again the catalytically active Fe-H species (**Scheme 10**, left).



Scheme 10. Postulated, simplified reaction mechanism for the iron-catalyzed formation of side-products **4** (right) and **5** (left) starting from olefin **1**. The heme-like porphyrin ligand around the iron center is not depicted for the sake of clarity. Si-H stands for any silane.

CONCLUSION

In summary, we have exploited an iron(III) catalyst that is highly active (190,000 TONs) and highly selective (up to 99% ketone selectivity for linear olefins) for the Wacker-type oxidation of olefins. The catalyst, which is based on the promiscuous activity encountered in several cytochromes from the P450 family, is built around a trivial porphyrin backbone containing carboxylic acid groups in the periphery. The role of the remote carboxylic acid groups belonging to heme-containing porphyrin studied in this work is likely to facilitate the stabilization of a key iron-hydride intermediate species in the catalytic cycle. In-depth substrate scope evaluation and mechanistic studies indicate the paramount importance of precisely fine-tuning the reaction conditions to control catalyst reactivity for the precise chemo-selective product formation. For instance, styrene derivatives lead to acetophenone derivatives (91-99%) when silanes were added as last reagents to the reaction mixture. If not, side-products resulting from ketone hydrogenation (alcohol formation) and unprecedented reductive olefin homo-coupling were significantly obtained. In the case of aliphatic olefins, minor formation of hydrogenated olefins were observed for challenging substrates besides major formation of ketone products (67-85%). Moreover, allyl-containing derivatives that are known to undergo oxidative C=C scission under similar reaction conditions, still afforded in the present case promising yields of ketone products (38-70%). The applicability of this protocol is demonstrated with the selective oxidation of a biologically-relevant indole to 2-oxindole without the requirements to use highly oxidizing agents. In addition, this iron catalyst exhibits temporal control of reactivity by switching the atmosphere or by sequential addition of bases and acids as well as recyclability and reusability properties. On the other hand, replacing silanes for more benign hydride sources is an important consideration in the search for more sustainable developments. Overall, the presented contribution points out that the rational design of iron catalysts is of relevance for disclosing highly selective transformations even if multiple catalytic cycles operate simultaneously. We anticipate that the bio-inspired iron catalyst studied here should find new applications in olefin functionalization³⁷ and as a building block for incorporation in solid supports or metal-organic frameworks³⁸ in view to disclose heterogeneous versions of the Wacker-type oxidation of olefins.

AUTHOR INFORMATION

Corresponding Author

* Rafael Gramage-Doria, Univ Rennes, CNRS, ISCR-UMR6226, F-35000 Rennes, France
 orcid.org/0000-0002-0961-4530
 Email: rafael.gramage-doria@univ-rennes1.fr

ASSOCIATED CONTENT

Supporting Information.

Experimental procedures, additional figures, and NMR spectra (PDF). "This material is available free of charge via the Internet at <http://pubs.acs.org>."

ACKNOWLEDGMENT

The CNRS, University of Rennes 1, Fondation Rennes 1 (MSc fellowship to K.Y. and S.K.) and Agence Nationale de la Recherche (ANR-19-CE07-0039, PhD fellowship to J.T.) are acknowledged for financial support.

CONFLICTS OF INTEREST

The authors are inventors of a deposited patent (EP 22 306 742.2) based on the research presented in this contribution.

REFERENCES

- (1) Smidt, J.; Hafner, W.; Jira, R.; Sedlmeier, J.; Sieber, R.; Rüttinger, R.; Kojer, H. Katalytische Umsetzungen von Olefinen an Platinmetall-Verbindungen Das Consortium-Verfahren zur Herstellung von Acetaldehyd. *Angew. Chem.* **1959**, *71*, 176-182.
- (2) (a) Keith, J. A.; Nielsen, R. J.; Oxgaard, J.; Goddard, W. A. Unraveling the Wacker Oxidation Mechanisms. *J. Am. Chem. Soc.* **2007**, *129*, 12342-12343. (b) Keith, J. A.; Henry, P. M. The Mechanism of the Wacker Reaction: A Tale of Two Hydroxypalladations. *Angew. Chem. Int. Ed.* **2009**, *48*, 9038-9049. (c) Kocovsky, P.; Backvall, J.-E. The *syn/anti*-Dichotomy in the Palladium-Catalyzed Addition of Nucleophiles to Alkenes. *Chem. Eur. J.* **2015**, *21*, 36-56. (d) Dong, J. J.; Browne, W. R.; Feringa, B. L. Palladium-Catalyzed *anti*-Markovnikov Oxidation of Terminal Alkenes. *Angew. Chem. Int. Ed.* **2015**, *54*, 734-744. (e) Baiju, T. V.; Gravel, E.; Doris, E.; Namboothiri, I. N. N. Recent developments in Tsuji-Wacker oxidation. *Tetrahedron Lett.* **2016**, *57*, 3993-4000. (f) Muzart, J. Progress in the synthesis of aldehydes from Pd-catalyzed Wacker-type reactions of terminal olefins. *Tetrahedron* **2021**, *87*, 132024.
- (3) (a) Hafner, W.; Jira, R.; Sedlmeier, J.; Smidt, J. Über die Reaktionen von Olefinen mit wäßrigen Lösungen von Palladiumsalzen. *Chem. Ber.* **1962**, *95*, 1575-1581. (b) Smidt, J.; Hafner, W.; Jira, R.; Sieber, R.; Sedlmeier, J.; Sabel, A. The Oxidation of Olefins with Palladium Chloride Catalysts. *Angew. Chem. Int. Ed.* **1962**, *1*, 80-88. (c) Jira, R. Acetaldehyde from Ethylene - A Retrospective on the Discovery of the Wacker Process. *Angew. Chem. Int. Ed.* **2009**, *48*, 9034-9037.
- (4) (a) Comas-Vives, A.; Stirling, A.; Lledós, A.; Ujaque, G. The Wacker Process: Inner- or Outer-Sphere Nucleophilic Addition? New Insights from Ab Initio Molecular Dynamics. *Chem. Eur. J.* **2010**, *16*, 8738-8747. (b) Sigman, M. S.; Werner, E. W. Imparting Catalyst Control upon Classical Palladium-Catalyzed Alkenyl C-H Bond Functionalization Reactions. *Acc. Chem. Res.* **2012**, *45*, 874-884. (c) Stirling, A.; Nair, N. N.; Lledo, A.; Ujaque, G. Challenges in modeling homogeneous catalysis: new answers from ab initio molecular dynamics to the controversy over the Wacker process. *Chem. Soc. Rev.* **2014**, *43*, 4940-4952. (d) Ura, Y. Palladium-Catalyzed Anti-Markovnikov Oxidation of Aromatic and Aliphatic Alkenes to Terminal Acetals and Aldehydes. *Synthesis* **2021**, *53*, 848-860. (e) Morandi, B.; Wickens, Z. K.; Grubbs, R. H. Practical and General Palladium-Catalyzed Synthesis of Ketones from Internal Olefins. *Angew. Chem. Int. Ed.* **2013**, *52*, 2944-2948. (f) Morandi, B.; Wickens, Z. K.; Grubbs, R. H. Regioselective Wacker Oxidation of Internal Alkenes: Rapid Access to Functionalized Ketones Facilitated by Cross-Metathesis. *Angew. Chem. Int. Ed.* **2013**, *52*, 9751-9754. (g) Wickens, Z. K.; Morandi, B.; Grubbs, R. H. Aldehyde-Selective Wacker-Type Oxidation of Unbiased Alkenes Enabled by a Nitrite Co-Catalyst. *Angew. Chem. Int. Ed.* **2013**, *52*, 11257-11260. (h) Hu, M.; Wu, W.; Jiang, H. Palladium-Catalyzed Oxidation Reactions of Alkenes with Green Oxidants. *ChemSusChem* **2019**, *12*, 2911-2935.
- (5) (a) Clement, W. H.; Selwitz, C. M. Improved Procedures for Converting Higher α -Olefins to Methyl Ketones with Palladium Chloride. *J. Org. Chem.* **1964**, *29*, 241-243. (b) Tsuji, J. Synthetic Applications of the Palladium-Catalyzed Oxidation of Olefins to Ketones. *Synthesis* **1984**, 369-384. (c) Tsuji, J.; Nagashima, H.; Nemoto, H. A GENERAL SYNTHETIC METHOD FOR THE PREPARATION OF METHYL KETONES FROM TERMINAL OLEFINS: 2-DECANONE. *Org. Synth.* **1984**, *62*, 9-13. (d) Takacs, J. M.; Jiang, X.-t. The Wacker Reaction and Related Alkene Oxidation Reactions. *Curr. Org. Chem.* **2003**, *7*, 369-396. (e) Cornell, C. N.; Sigman, M. S. Recent Progress in Wacker Oxidations: Moving toward Molecular Oxygen as the Sole Oxidant. *Inorg. Chem.* **2007**, *46*, 1903-1909. (f) Wang, D.; Weinstein, A. B.; White, P. B.; Stahl, S. S. Ligand-Promoted Palladium-Catalyzed Aerobic Oxidation Reactions. *Chem. Rev.* **2018**, *118*, 2636-2679. (g) Ura, Y. Realization of Anti-Markovnikov Selectivity in Pd-Catalyzed Oxidative Acetalization and Wacker-Type Oxidation of Terminal Alkenes. *Chem. Rec.* **2021**, *21*, 3458-3469.
- (6) (a) Bolm, C.; Legros, J.; Le Pailh, J.; Zani, L. Iron-Catalyzed Reactions in Organic Synthesis. *Chem. Rev.* **2004**, *104*, 6217-6254. (b) *Catalysis without Precious Metals* (Ed.: Bullcock, R. M.), Wiley-VCH, Weinheim, **2010**. (c) Bauer, I.; Knölker, H.-J. Iron Catalysis in Organic Synthesis. *Chem. Rev.* **2015**, *115*, 3170-3387. (d) Egorova, K. S.; Ananikov, V. P. Which Metals are Green for Catalysis? Comparison of the Toxicities of Ni, Cu, Fe, Pd, Pt, Rh, and Au Salts. *Angew. Chem. Int. Ed.* **2016**, *55*, 12150-12162. (e) Fürstner, A. Iron Catalysis in Organic Synthesis: A Critical Assessment of What It Takes To Make This Base Metal a Multitasking Champion. *ACS Cent. Sci.* **2016**, *2*, 778-789. (f) Bauer, E. B. Recent Advances in Iron Catalyzed Oxidation Reactions of Organic Compounds. *Isr. J. Chem.* **2017**, *57*, 1131-1150. (g) Rana, S.; Biswas, J. P.; Paul, S.; Paik, A.; Maiti, D. Organic synthesis with the most abundant transition metal-iron: from rust to multitasking catalysts. *Chem. Soc. Rev.* **2021**, *50*, 243-472.
- (7) (a) Fernandes, R. A.; Jha, A. K.; Kumar, P. Recent advances in Wacker oxidation: from conventional to modern variants and applications. *Catal. Sci. Technol.* **2020**, *10*, 7448-7470. (b) Rajeshwaran, P.; Trouvé, J.; Youssef, K.; Gramage-Doria, R. Sustainable Wacker-Type Oxidations. *Angew. Chem. Int. Ed.* **2022**, *61*, e202211016.
- (8) (a) Chen, G.-Q.; Xu, Z.-J.; Zhou, C.-Y.; Che, C.-M. Selective oxidation of terminal aryl and aliphatic alkenes to aldehydes catalyzed by iron(III) porphyrins with triflate as a counter anion. *Chem. Commun.* **2011**, *47*, 10963-10965. (b) Du, Y.-D.; Tse, C.-W.; Xu, Z.-J.; Liu, Y.; Che, C.-M. [Fe^{III}(TF₄DMAP)OTf] catalysed anti-Markovnikov oxidation of terminal aryl alkenes to aldehydes and transformation of methyl aryl tertiary amines to formamides with H₂O₂ as a terminal oxidant. *Chem. Commun.* **2014**, *50*, 12669-12672.
- (9) (a) Hammer, S. C.; Kubik, G.; Watkins, E.; Huang, S.; Minges, H.; Arnold, F. H. Anti-Markovnikov alkene oxidation by metal-oxo-mediated enzyme catalysis. *Science* **2017**, *358*, 215-218. (b) Soler, J.; Gergel, S.; Klaus, C.; Ham-

- mer, S. C.; Garcia-Borràs, M. Enzymatic Control over Reactive Intermediates Enables Direct Oxidation of Alkenes to Carbonyls by a P450 Iron-Oxo Species. *J. Am. Chem. Soc.* **2022**, *144*, 15954-15968. (c) Zhang, G.; Hu, X.; Chiang, C.-W.; Yi, H.; Pei, P.; Singh, A. K.; Lei, A. Anti-Markovnikov Oxidation of β -Alkyl Styrenes with H₂O as the Terminal Oxidant. *J. Am. Chem. Soc.* **2016**, *138*, 12037-12040.
- (10) (a) Liu, B.; Jin, F.; Wang, T.; Yuan, X.; Han, W. Wacker-Type Oxidation Using an Iron Catalyst and Ambient Air: Application to Late-Stage Oxidation of Complex Molecules. *Angew. Chem. Int. Ed.* **2017**, *56*, 12712-12717. (b) Liu, B.; Han, W. Iron-Catalyzed Wacker-Type Oxidation. *Synlett* **2018**, *29*, 383-387. (c) Puls, F.; Knölker, H.-J. Conversion of Olefins into Ketones by an Iron-Catalyzed Wacker-type Oxidation Using Oxygen as the Sole Oxidant. *Angew. Chem. Int. Ed.* **2018**, *57*, 1222-1226. (d) Puls, F.; Seewald, F.; Grinenko, V.; Klauß, H.-H.; Knölker, H.-J. Mechanistic Studies on the Hexadecafluorophthalocyanine-Iron-Catalyzed Wacker-Type Oxidation of Olefins to Ketones. *Chem. Eur. J.* **2021**, *27*, 16776-16787. (e) Puls, F.; Linke, P.; Kataeva, O.; Knölker, H.-J. Iron-Catalyzed Wacker-type Oxidation of Olefins at Room Temperature with 1,3-Diketones or Neocuproine as Ligands. *Angew. Chem. Int. Ed.* **2021**, *60*, 14083-14090. (f) Schuh, T.; Kataeva, O.; Knölker, H.-J. μ -Oxo-bis[*octacosafuoro-meso-tetraphenylporphyrinato*iron(III)] – synthesis, crystal structure, and catalytic activity in oxidation reactions. *Chem. Sci.* **2023**, *14*, 257-265
- (11) (a) Mansuy, D.; Leclaire, J.; Fontcave, M.; Momenteau, M. Oxidation of monosubstituted olefins by cytochromes P-450 and heme models: Evidence for the formation of aldehydes in addition to epoxides and allylic alcohols. *Biochem. Biophys. Res. Commun.* **1984**, *119*, 319-325. (b) de Visser, S. P.; Kumar, D.; Shaik, S. How do aldehyde side products occur during alkene epoxidation by cytochrome P450? Theory reveals a state-specific multi-state scenario where the high-spin component leads to all side products. *J. Inorg. Biochem.* **2004**, *98*, 1183-1193. (c) Yin, Y.-C.; Yu, H.-L.; Luan, Z.-J.; Li, R.-J.; Ouyang, P.-F.; Liu, J.; Xu, J.-H. Unusually Broad Substrate Profile of Self-Sufficient Cytochrome P450 Monooxygenase CYP116B4 from *Labrenzia aggregata*. *ChemBioChem* **2014**, *15*, 2443-2449. (d) Guengerich, F. P.; Munro, A. W. Unusual cytochrome p450 enzymes and reactions. *J. Biol. Chem.* **2013**, *288*, 17065-17073. (e) Kazlauskas, R. J. Enhancing catalytic promiscuity for biocatalysis. *Curr. Opin. Chem. Biol.* **2005**, *9*, 195-201.
- (12) (a) Shimizu, T.; Lengalova, A.; Martinek, V.; Martinkova, M. Heme: emergent roles of heme in signal transduction, functional regulation and as catalytic centres. *Chem. Soc. Rev.* **2019**, *48*, 5624-5657. (b) Dong, J.; Fernandez-Fueyo, E.; Hollmann, F.; Paul, C. E.; Pesic, M.; Schmidt, S.; Wang, Y.; Younes, S.; Zhang, W. Biocatalytic Oxidation Reactions: A Chemist's Perspective. *Angew. Chem. Int. Ed.* **2018**, *57*, 9238-9261. (c) Wu, S.; Zhou, Y.; Li, Z. Biocatalytic selective functionalisation of alkenes *via* single-step and one-pot multi-step reactions. *Chem. Commun.* **2019**, *55*, 883-896. (d) Huang, X.; Groves, J. T. Oxygen Activation and Metalloporphyrins. *Chem. Rev.* **2018**, *118*, 2491-2553. (e) Guengerich, F. P. Mechanisms of Cytochrome P450-Catalyzed Oxidations. *ACS Catal.* **2018**, *8*, 10964-10976. (f) Ciaramella, A.; Catucci, G.; Gilardi, G.; Di Nardo, G. Crystal structure of bacterial CYP116B5 heme domain: New insights on class VII P450s structural flexibility and peroxxygenase activity. *Int. J. Biol. Macromol.* **2019**, *140*, 577-587. (g) Denisov, I. G.; Makris, T. M.; Sligar, S. G.; Schlichting, I. Structure and Chemistry of Cytochrome P450. *Chem. Rev.* **2005**, *105*, 2253-2277. (h) Liu, J.; Chakraborty, S.; Hosenzadeh, P.; Yu, Y.; Tian, S.; Petrik, I.; Bhagi, A.; Lu, Y. Metalloproteins Containing Cytochrome, Iron-Sulfur, or Copper Redox Centers. *Chem. Rev.* **2014**, *114*, 4366-4469. (i) Krest, C. M.; Onderko, E. L.; Yosca, T. H.; Calixto, J. C.; Karp, R. F.; Livada, J.; Rittle, J.; Green, M. T. Reactive intermediates in cytochrome p450 catalysis. *J. Biol. Chem.* **2013**, *288*, 17074-17081. (j) Fürst, M. J. L. J.; Fiorentini, F.; Fraaije, M. W. Beyond active site residues: overall structural dynamics control catalysis in flavin-containing and heme-containing monooxygenases. *Curr. Opin. Struct. Biol.* **2019**, *59*, 29-37.
- (13) (a) Reid, L. S.; Mauk, M. R.; Mauk, A. G. Role of heme propionate groups in cytochrome b5 electron transfer. *J. Am. Chem. Soc.* **1984**, *106*, 2182-2185. (b) Reid, L. S.; Lim, A. R.; Mauk, A. G. Role of heme vinyl groups in cytochrome b5 electron transfer. *J. Am. Chem. Soc.* **1986**, *108*, 8197-8201. (c) Lee, K.-B.; La Mar, G. N.; Pandey, R. K.; Rezzano, I. N.; Mansfield, K. E.; Smith, K. M.; Pochapsky, T. C.; Sligar, S. G. Proton NMR study of the role of heme carboxylate side chains in modulating heme pocket structure and the mechanism of reconstitution of cytochrome b5. *Biochemistry* **1991**, *30*, 1878-1887. (d) Warren, J. J.; Mayer, J. M. Proton-Coupled Electron Transfer Reactions at a Heme-Propionate in an Iron-Protoporphyrin-IX Model Compound. *J. Am. Chem. Soc.* **2011**, *133*, 8544-8551. (e) Deng, Y.; Weaver, M. L.; Hoke, K. R.; Pletneva, E. V. A Heme Propionate Staples the Structure of Cytochrome c for Methionine Ligation to the Heme Iron. *Inorg. Chem.* **2019**, *58*, 14085-14106.
- (14) (a) Qi, X.; Kohler, D. G.; Hull, K. L.; Liu, P. Energy Decomposition Analyses Reveal the Origins of Catalyst and Nucleophile Effects on Regioselectivity in Nucleopalladation of Alkenes. *J. Am. Chem. Soc.* **2019**, *141*, 11892-11904. (b) Bullock, R. M.; Chen, J. G.; Gagliardi, L.; Chirik, P. J.; Farha, O. K.; Hendon, C. H.; Jones, C. W.; Keith, J. A.; Klosin, J.; Minter, S. D.; Morris, R. H.; Radosevich, A. T.; Rauchfuss, T. B.; Strotman, N. A.; Vojvodic, A.; Ward, T. R.; Yang, J. Y.; Surendranath, Y. Using nature's blueprint to expand catalysis with Earth-abundant metals. *Science* **2020**, *369*, eabc3183.
- (15) Kasemthaveechok, S.; Fabre, B.; Loget, G.; Gramage-Doria, R. Remote ion-pair interactions in Fe-porphyrin-based molecular catalysts for the hydrogen evolution reaction. *Catal. Sci. Technol.* **2019**, *9*, 1301-1308.
- (16) See details in the Supporting Information.
- (17) Kurtz, Jr., D. M. Oxo- and hydroxo-bridged diiron complexes: a chemical perspective on a biological unit. *Chem. Rev.* **1990**, *90*, 585-606.
- (18) A mechanism for the formation of Fe-2 from Fe-1 is proposed in Scheme S5 in the Supporting Information.
- (19) The reaction rate at 50 °C is 1.02 x 10⁻⁷ mol.s⁻¹ while the reaction rate at 0 °C is 1.59 x 10⁻⁸ mol.s⁻¹, see reference 16.
- (20) A mechanism for the formation of 4b is proposed in Scheme S7 in the Supporting Information in agreement with reference 21.
- (21) (a) Lo, J. C.; Gui, J.; Yabe, Y.; Pan, C.-M.; Baran, P. S. Functionalized olefin cross-coupling to construct carbon-carbon bonds. *Nature* **2014**, *516*, 343-348. (b) Lo, J. C.; Yabe, Y.; Baran, P. S. A Practical and Catalytic Reductive Olefin Coupling. *J. Am. Chem. Soc.* **2014**, *136*, 1304-1307. (c) Dao, H. T.; Li, C.; Michaudel, Q.; Maxwell, B. D.; Baran, P. S. Hydromethylation of Unactivated Olefins. *J. Am. Chem. Soc.* **2015**, *137*, 8046-8049. (d) Lo, J. C.; Kim, D. Y.; Pan, C.-M.; Edwards, J. T.; Yabe, Y.; Gui, J. H.; Qin, T.; Gutierrez, S.; Giacoboni, J.; Smith, M. W.; Holland, P. L.; Baran, P. S.

- Fe-Catalyzed C–C Bond Construction from Olefins via Radicals. *J. Am. Chem. Soc.* **2017**, *139*, 2484–2503. (e) Kim, D.; Wahidur Rahaman, S. M.; Mercado, B. Q.; Poli, R.; Holland, P. L. Roles of Iron Complexes in Catalytic Radical Alkene Cross-Coupling: A Computational and Mechanistic Study. *J. Am. Chem. Soc.* **2019**, *141*, 7473–7485. (f) Green, S. A.; Crossley, S. W. M.; Matos, J. L. M.; Vásquez-Céspedes, S.; Shevick, S. L.; Shenvi, R. A. The High Chemofidelity of Metal-Catalyzed Hydrogen Atom Transfer. *Acc. Chem. Res.* **2018**, *51*, 2628–2640. (g) Jiang, H.; Lai, W.; Chen, H. Generation of Carbon Radical from Iron-Hydride/Alkene: Exchange-Enhanced Reactivity Selects the Reactive Spin State. *ACS Catal.* **2019**, *9*, 6080–6086. (h) Shevick, S. L.; Wilson, C. V.; Kotesova, S.; Kim, D.; Holland, P. L.; Shenvi, R. A. Catalytic hydrogen atom transfer to alkenes. *Chem. Sci.* **2020**, *11*, 12401–12422. (i) Sarkar, S.; Cheung, K. P. S.; Gevorgyan, V. C–H functionalization reactions enabled by hydrogen atom transfer to carbon-centered radicals. *Chem. Sci.* **2020**, *11*, 12974–12993. (j) Kattamuri, P. V.; West, J. G. Hydrogenation of Alkenes via Cooperative Hydrogen Atom Transfer. *J. Am. Chem. Soc.* **2020**, *142*, 19316–19326.
- (22) Note that the isolated yields of ketone products **2** in some cases were lower than the reported GC yields (using dodecane as internal standard) due to the low boiling point of these compounds, see reference 16.
- (23) For examples of selective iron-catalyzed epoxidation of olefins, see: Mas-Ballesté, R.; Que, L. Iron-Catalyzed Olefin Epoxidation in the Presence of Acetic Acid: Insights into the Nature of the Metal-Based Oxidant. *J. Am. Chem. Soc.* **2007**, *129*, 15964–15972. (b) Hasan, K.; Brown, N.; Kozak, C. M. Iron-catalyzed epoxidation of olefins using hydrogen peroxide. *Green Chem.* **2011**, *13*, 1230–1237.
- (24) Gonzalez-de-Castro, A.; Xiao, J. L. Green and Efficient: Iron-Catalyzed Selective Oxidation of Olefins to Carbonyls with O₂. *J. Am. Chem. Soc.* **2015**, *137*, 8206–8218.
- (25) Liu, B.; Hu, P.; Xu, F.; Cheng, L.; Tan, M.; Han, W. Nickel-catalyzed remote and proximal Wacker-type oxidation. *Commun. Chem.* **2019**, *2*, 5.
- (26) (a) Leone, L.; D'Alonzo, D.; Maglio, O.; Pavone, V.; Nastri, F.; Lombardi, A. Highly Selective Indole Oxidation Catalyzed by a Mn-Containing Artificial. *ACS Catal.* **2021**, *11*, 9407–9417. (b) Mondal, P.; Rajapakse, S.; Wijeratne, G. B. Following Nature's Footprint: Mimicking the High-Valent Heme-Oxo Mediated Indole Monooxygenation Reaction Landscape of Heme Enzymes. *J. Am. Chem. Soc.* **2022**, *144*, 3843–3854.
- (27) (a) Dalgliesh, C. E.; Kelly, W. Direct oxidation of indoles to oxindoles. *J. Chem. Soc.* **1958**, 3726–3727. (b) Jiang, X.; Zheng, C.; Lei, L.; Lin, K.; Yu, C. Synthesis of 2-Oxindoles from Substituted Indoles by Hypervalent-Iodine Oxidation. *Eur. J. Org. Chem.* **2018**, 1437–1442. (c) Shelar, S. V.; Argade, N. P. Regioselective oxidation of indoles to 2-oxindoles. *Org. Biomol. Chem.* **2019**, *17*, 6671–6677. (d) Xu, J.; Lian, L.; Zheng, H.; Chi, Y. R.; Tong, R. Green oxidation of indoles using halide catalysis. *Nature Commun.* **2019**, *10*, 4754. (e) Zhao, G.; Liang, L.; Wang, E.; Lou, S.; Qi, R.; Tong, R. Fenton chemistry enables the catalytic oxidative rearrangement of indoles using hydrogen peroxide. *Green Chem.* **2021**, *23*, 2300–2307. (f) Liang, P.; Zhao, H.; Zhou, T.; Zeng, K.; Jiao, W.; Pan, Y.; Liu, Y.; Fang, D.; Ma, X.; Shao, H. Rapid Oxidation Indoles into 2-Oxindoles Mediated by PIFA in Combination with n-Bu₄NCl·H₂O. *Adv. Synth. Catal.* **2021**, *363*, 3532–3538. (g) Mintz, T.; More, N. Y.; Gaster, E.; Pappo, D. Iron-Catalyzed Oxidative Cross-Coupling of Phenols and Tyrosine Derivatives with 3-Alkyl-oxindoles. *J. Org. Chem.* **2021**, *86*, 18164–18178.
- (28) (a) Kaur, M. *Key Heterocycle Cores for Designing Multitargeting Molecules* (Ed.: O. Silakari), Elsevier, **2018**; pp 211–246. (b) Kaur, M.; Singh, M.; Chadha, N.; Silakari, O. Oxindole: A chemical prism carrying plethora of therapeutic benefits. *Eur. J. Med. Chem.* **2016**, *123*, 858–894. (c) Peddibhotla, S. 3-Substituted-3-hydroxy-2-oxindole, an Emerging New Scaffold for Drug Discovery with Potential Anti-Cancer and other Biological Activities. *Curr. Bioact. Compd.* **2009**, *5*, 20–38. (d) Khetmalis, Y. M.; Shivani, M.; Murugesan, S.; Sekhar, K. V. G. C. Oxindole and its derivatives: A review on recent progress in biological activities. *Biomed. Pharmacother.* **2021**, *141*, 111842.
- (29) Bhugun, I.; Lexa, D.; Savéant, J.-M. Homogeneous Catalysis of Electrochemical Hydrogen Evolution by Iron(o) Porphyrins. *J. Am. Chem. Soc.* **1996**, *118*, 3982–3983.
- (30) For the spectroscopic characterization of iron-hydride species in the context of other type of catalysis, see: (a) Kazlauskas, R. J.; Wrighton, M. S. Photochemistry of alkylideneiron(*η*⁵-cyclopentadienyl)iron and -ruthenium. Ligand substitution and alkene elimination via photogenerated sixteen-valence-electron intermediates. *Organometallics* **1982**, *1*, 602–611. (b) Knölker, H.-J.; Baum, E.; Goesmann, H.; Klauss, R. Demetalation of Tricarbonyl(cyclopentadienone)iron Complexes Initiated by a Ligand Exchange Reaction with NaOH—X-Ray Analysis of a Complex with Nearly Square-Planar Coordinated Sodium. *Angew. Chem. Int. Ed.* **1999**, *38*, 2064–2066. (c) Gorgas, N.; Stöger, B.; Pittenauer, E.; Allmaier, G.; Veiros, L. F.; Kirchner, K. Efficient Hydrogenation of Ketones and Aldehydes Catalyzed by Well-Defined Iron(II) PNP Pincer Complexes: Evidence for an Insertion Mechanism. *Organometallics* **2014**, *33*, 6905–6914. (d) Mastalir, M.; Glatz, M.; Gorgas, N.; Stöger, B.; Pittenauer, E.; Allmaier, G.; Veiros, L. F.; Kirchner, K. Divergent Coupling of Alcohols and Amines Catalyzed by Isoelectronic Hydride Mn^I and Fe^{II} PNP Pincer Complexes. *Chem. Eur. J.* **2016**, *22*, 12316–12320. (e) Gorgas, N.; Stöger, B.; Veiros, L. F.; Kirchner, K. Highly Efficient and Selective Hydrogenation of Aldehydes: A Well-Defined Fe(II) Catalyst Exhibits Noble-Metal Activity. *ACS Catal.* **2016**, *6*, 2664–2672. (f) Bertini, F.; Gorgas, N.; Stöger, B.; Peruzzini, M.; Veiros, L. F.; Kirchner, K.; Gonsalvi, L. Efficient and Mild Carbon Dioxide Hydrogenation to Formate Catalyzed by Fe(II) Hydrido Carbonyl Complexes Bearing 2,6-(Diaminopyridyl)diphosphine Pincer Ligands. *ACS Catal.* **2016**, *6*, 2889–2893. (g) Jiang, S.; Quintero-Duque, S.; Roisnel, T.; Dorcet, V.; Grelhier, M.; Sabo-Etienne, S.; Darcel, C.; Sortais, J.-B. Direct synthesis of dicarbonyl PCP-iron hydride complexes and catalytic dehydrogenative borylation of styrene. *Dalton Trans.* **2016**, *45*, 11101–11108.
- (31) Wayland, B. B.; Van Voorhees, S. L.; Wilker, C. Organometallic Chemistry of Rhodium Tetraphenylporphyrin Derivatives: Formyl, Hydroxymethyl, and Alkyl Complexes. *Inorg. Chem.* **1986**, *25*, 4039–4042. (b) Wayland, B. B.; Ba, S.; Sherry, A. E. Activation of Methane and Toluene by Rhodium(II) Porphyrin Complexes. *J. Am. Chem. Soc.* **1991**, *113*, 5305–5311. (c) Collman, J. P.; Boulatov, R. Synthesis and Reactivity of Porphyrinorhodium(II)-Triethylphosphine Adducts: The Role of Pe₃ in Stabilizing a Formal Rh(II) State. *J. Am. Chem. Soc.* **2000**, *122*, 11812–11821.
- (32) Fulmer, G. R.; Miller, A. J. M.; Sherden, N. H.; Gottlieb, H. E.; Nudelman, A.; Stoltz, B. M.; Bercaw, J. E.; Goldberg, K. I. NMR Chemical Shifts of Trace Impurities: Common Laboratory Solvents, Organics, and Gases in Deuterated Solvents Relevant to the Organometallic Chemist. *Organometallics* **2010**, *29*, 2176–2179.

- (33) (a) Moineau, J.; Granier, M.; Lanneau, G. F. Organized Self-Assembled Monolayers from Organosilanes Containing Rigid π -Conjugated Aromatic Segments. *Langmuir* **2004**, *20*, 3202-3207. (b) Leong, B.-X.; Teo, Y.-C.; Condamines, C.; Yang, M.-C.; Su, M.-D.; So, C.-W. A NHC-Silyliumylidene Cation for Catalytic N-Formylation of Amines Using Carbon Dioxide. *ACS Catal.* **2020**, *10*, 14824-14833.
- (34) John, J.; Gravel, E.; Hagège, A.; Li, H.; Gacoin, T.; Doris, E. Catalytic Oxidation of Silanes by Carbon Nanotube-Gold Nanohybrids. *Angew. Chem. Int. Ed.* **2011**, *50*, 7533-7536.
- (35) Other analysis (^{13}C NMR, ^{29}Si NMR, DOSY NMR, HMBC NMR, NOESY NMR, FT-IR, UV-vis and HRMS spectroscopy) were performed but failed to give a stable signal through the analysis. X-ray crystallography studies failed so far and further analysis (EPR, Mossbauer, DFT, etc.) devoted to fully characterize such iron-hydride species will be reported at due time and it is beyond the scope of the current contribution.
- (36) (a) Mukaiyama, T.; Yamada, T. Recent Advances in Aerobic Oxygenation. *Bull. Chem. Soc. Jpn.* **1995**, *68*, 17-35. (b) Mukaiyama, T.; Isayama, S.; Inoki, S.; Kato, K.; Yamada, T.; Takai, T. Oxidation-Reduction Hydration of Olefins with Molecular Oxygen and 2-Propanol Catalyzed by Bis(acetylacetonato)cobalt(II). *Chem. Lett.* **1989**, 449-452. (c) Isayama, S.; Mukaiyama, T. A New Method for Preparation of Alcohols from Olefins with Molecular Oxygen and Phenylsilane by the Use of Bis(acetylacetonato)cobalt(II). *Chem. Lett.* **1989**, 1071-1074.
- (37) (a) Tang, S.; Liu, K.; Liu, C.; Lei, A. Olefinic C-H functionalization through radical alkenylation. *Chem. Soc. Rev.* **2015**, *44*, 1070-1082. (b) Crossley, S. W. M.; Obradors, C.; Martinez, R. M.; Shenvi, R. A. Mn-, Fe-, and Co-Catalyzed Radical Hydrofunctionalizations of Olefins. *Chem. Rev.* **2016**, *116*, 8912-9000. (c) Dong, Z.; Ren, Z.; Thompson, S. J.; Xu, Y.; Dong, G. Transition-Metal-Catalyzed C-H Alkylation Using Alkenes. *Chem. Rev.* **2017**, *117*, 9333-9403. (d) Lan, X.-W.; Wang, N.-X.; Xing, Y. Recent Advances in Radical Difunctionalization of Simple Alkenes. *Eur. J. Org. Chem.* **2017**, 5821-5851. (e) Jiang, H.; Studer, A. Intermolecular radical carboamination of alkenes. *Chem. Soc. Rev.* **2020**, *49*, 1790-1811. (f) Patel, M.; Desai, B.; Sheth, A.; Dholakiya, B. Z.; Naveen, T. Recent Advances in Mono- and Difunctionalization of Unactivated Olefins. *Asian J. Org. Chem.* **2021**, 3201-3232.
- (38) (a) Durot, S.; Taesch, J.; Heitz, V. Multiporphyrinic Cages: Architectures and Functions. *Chem. Rev.* **2014**, *114*, 8542-8585. (b) Zhang, X.; Wasson, M. C.; Shayan, M.; Berdichevsky, E. K.; Ricardo-Noordberg, J.; Singh, Z.; Papazyan, E. K.; Castro, A. J.; Marino, P.; Ajoyan, Z.; Chen, Z.; Islamoglu, T.; Howarth, A. J.; Liu, Y.; Majewski, M. B.; Katz, M. J.; Mondloch, J. E.; Farha, O. K. A historical perspective on porphyrin-based metal-organic frameworks and their applications. *Coord. Chem. Rev.* **2021**, *429*, 213615.

Table of Contents artwork

